Computer study of the spectral characteristics of the disperse water–methane system

A. Y. Galashev†

Institute of Industrial Ecology, Ural Branch, Russian Academy of Sciences 62099, *S. Kovalevskaya Str.*, 20, *Yekaterinburg, Russia*

(Received 1 April 2013; revised manuscript received 6 May 2013)

The interaction of water clusters that adsorbed methane molecules with infrared radiation is studied by molecular dynamics. The presence of methane molecules in the disperse water system leads to an increase in absorption and emission of infrared radiation and a strong depletion of the Raman spectrum. In this case, the reflection coefficient of a monochromatic plane electromagnetic wave increases and its frequency spectrum significantly changes. The comparison of experimental data for similar characteristics of water, methane, or their mixtures is presented.

Keywords: adsorption, methane, water cluster, infrared and Raman spectra

PACS: 36.40.Mr, 36.20.Ng, 92.70.Cp, 92.70.Er **DOI:** 10.1088/1674-1056/22/12/123602

1. Introduction

Methane is the most abundant reactive trace gas in the atmosphere and arises from both natural and anthropogenic sources. Methane is removed from the atmosphere (i.e., converted into less harmful products) by a range of chemical and biological processes, which occur in different regions of the atmosphere. These include tropospheric oxidation, stratospheric oxidation, and absorption by soils. Infrared (IR) spectroscopy is the best diagnostic instrument for studying methane in the environment. Due to the high symmetry of a methane molecule, its complex electron structure arises from closely spaced levels.[1] The frequencies of four normal modes of methane are related approximately as follows: $\nu_1 \approx \nu_3 \approx 2\nu_2 \approx 2\nu_4$. As water is almost universal in the Solar System,[2] the methane–water contacts change the spectroscopic characteristics of methane. The sum of the spectra of pure materials is known to differ from the spectrum of their mixture.[3] For example, the interaction of CH_4 with H_2O on the molecular level is accompanied by significant changes in the positions of peaks and spectral profiles in the near and middle IR regions.[3,4] Therefore, in order to explain the spectra of objects located outside the Solar System, we need to record spectra of CH_4 and H_2O upon their intermolecular interaction.

Methane–water systems play important roles in the practical application of organic fuel (in the form of clathrates), conversion of solar energy (thermochemistry), or methane formation in fermentation reactions.[5] Under environmental conditions, the free energy of hydration of small nonpolar molecules, such as methane, is mainly determined by the entropy component and depends, to a greater extent, on the number of the types of arrangement of all water molecules in a hydrate layer of methane rather than on their energy.[6] In the vicinity of small nonpolar molecules, water molecules can rearrange themselves to encapsulate a guest molecule and reform ruptured H bonds.[7,8]

To date, the main attention has been focused on studying the properties of extended liquid solutions and hydrates of methane (water ices containing large amounts of methane) and little work has dealt with the cluster hydrophobic effect in the atmosphere.[9–11] Small water clusters composed of 10 and 20 molecules have been considered in those studies. Water molecules have been shown to be immiscible with adsorbed methane molecules.

The aim of this work is to study the changes that take place in IR and Raman spectra upon methane adsorption on water clusters.

2. Computer model

The interaction between water molecules in clusters was described by a nonadditive potential, the additive component of which was represented by the modified[12] TIP4P potential for water,[13] while the nonadditive component was determined by the polarization interaction.[14] Thus, the potential energy of the system is described in the following manner:

$$U_{\rm tot} = U_{\rm pair} + U_{\rm pol},$$

where the pair component of the potential energy is determined by the Lennard–Jones and Coulomb contributions as follows:

$$U_{\rm pair} = \sum_i \sum_j \left[4\varepsilon^{\rm LJ} \left\{ \left(\frac{\sigma_{ij}^{\rm LJ}}{r_{ij}} \right)^{12} - \left(\frac{\sigma_{ij}^{\rm LJ}}{r_{ij}} \right)^{6} \right\} + \frac{q_i q_j}{r_{ij}} \right].$$

Here, r_{ij} is the distance between atoms i and j, q is the electric charge, and $\sigma^{\rm LJ}$ and $\varepsilon^{\rm LJ}$ are the Lennard–Jones potential parameters.[12]

†Corresponding author. E-mail: galashev@ecko.uran.ru

© 2013 Chinese Physical Society and IOP Publishing Ltd

Polarization energy is determined in the following way:

$$U_{\text{pol}} = -\frac{1}{2}\sum_i \boldsymbol{d}_i \cdot \boldsymbol{E}_i^0,$$

where $\boldsymbol{d}_i$ is the induced dipole moment of molecule i, $\boldsymbol{E}_i^0$ is the electric field strength generated by a system of fixed charges at a point of molecule i localization.[12]

The methane–methane interatomic interactions are determined by the Lennard–Jones and Coulomb contributions as follows:

$$\Phi_{ij}(r) = \varepsilon_{ij}\left[\left(\frac{r_0}{r_{ij}}\right)^{12} - 2\left(\frac{r_0}{r_{ij}}\right)^{6}\right] + \frac{q_i q_j}{r_{ij}}.$$

The magnitudes of parameters ε_{ij}, r_0, and q_i of H and C atoms in the CH_4 molecule are taken to be equal to 0.159 kJ/mol, 0.28525 nm, and 0.119e and 0.309 kJ/mol, 0.430 nm, and –0.476e, respectively.[15] The parameters of the Lennard–Jones potential that describes the methane–water interactions are found by the Berthelot–Lorentz formulas

$$\varepsilon_{mw}^{(\text{LJ})} = \sqrt{\varepsilon_m^{(\text{LJ})}\varepsilon_w^{(\text{LJ})}}, \quad \sigma_{mw}^{(\text{LJ})} = \frac{\sigma_m^{(\text{LJ})} + \sigma_w^{(\text{LJ})}}{2},$$

where $\varepsilon_m^{(\text{LJ})}$ and $\varepsilon_w^{(\text{LJ})}$ are the energy parameters and $\sigma_m^{(\text{LJ})}$ and $\sigma_w^{(\text{LJ})}$ are the geometric parameters of the potential for C and H atoms of the methane molecule and O atom of the water molecule, respectively.[9]

The trajectories of the mass centers of the molecules are determined by the fourth-order Gear method.[16] Time step Δt of integration is 0.2×10^{-16} s. In a molecular dynamics calculation of $2 \times 10^6 \Delta t$ long, the equilibration is preliminarily performed at $T = 233$ K for pure water clusters free of impurity molecules. The $(H_2O)_{50}$ cluster configuration at the 40-ps time moment is further used as the initial configuration for simulating $(CH_4)_i(H_2O)_{50}$ heteroclusters with $1 \leq i \leq 6$. Each added CH_4 molecule is initially placed into a position such that the shortest distance between the atoms of this molecule and atoms of water molecules is nearly 0.6 nm. At the beginning, the mass centers of CH_4 molecules are placed on the coordinate axes outside the water cluster. The initial orientation of methane molecules is arbitrary. A newly formed cluster is equilibrated within a time interval of $1.2 \times 10^6 \Delta t$ at $T = 233$ K; after that, the desired physicochemical properties are calculated at the same temperature within an interval of $2.5 \times 10^6 \Delta t$. A system of $(CH_4)_i(H_2O)_{50}$ clusters is formed in accordance with cluster statistical weights, which are determined as follows. We consider the case of unpolarized light scattering, when free path l of molecules is much shorter than light wavelength λ. Extinction (attenuation) ratio h of an incident beam is determined by, on the one hand, the Rayleigh formula,[17] and, on the other hand, scattering coefficient $\rho(h = 16\pi/3\rho)$ under an approximation of the scattering angle of 90°.[18] Taking into account that $h = \alpha + \rho$, where α is the absorption coefficient, we have

$$N = \frac{2\omega^4}{3\pi c^4}\frac{(\sqrt{\varepsilon}-1)^2}{\alpha}\left(1 - \frac{3}{16\pi}\right),$$

where N is the number of scattering centers per cubic centimeter, c is the speed of light, ε is medium dielectric permittivity, and ω is the frequency of the incident wave.

We define the following types of ultradisperse systems: system I is a monodisperse system of $(H_2O)_{50}$ clusters, system II is a region filled with water clusters having sizes of 10–50 molecules (the number of molecules in a cluster is increased with step $\Delta n = 5$), and system III is a medium composed of $(H_2O)_{50}$ clusters, each of which contains 1–6 adsorbed CH_4 molecules.

We form these systems in a manner such that a cluster containing i admixture molecules and n water molecules has the following statistical weight:

$$W_{in} = \frac{N_{in}}{N_{l\Sigma}}, \quad 1 \leq i \leq 6, \quad 10 \leq n \leq 50\ (\Delta n = 5),$$

where N_{in} is the number of clusters containing n water molecules and i CH_4 molecules in 1 cm^3, and l acquires values of 1 and 2:

$$N_{1\Sigma} = \sum_{n=1}^{9} N_{i=0,n}, \quad N_{2\Sigma} = \sum_{i=1}^{6} N_{i,n=50}.$$

Thereafter, all spectral characteristics are calculated with regard to accepted statistical weights W_{in}.

The motion equations for molecular rotation are analytically solved using the Rodrigues–Hamilton parameters,[19] and the integration of equations of motion involving rotations is implemented according to the Sonnenschein approach.[20]

3. Dielectric properties

The static dielectric constant ε_0 is calculated through the fluctuations of the total dipole moment,[21] and the complex value $\varepsilon(\omega)$ is determined through the autocorrelation function of the total dipole moment of a cluster.[22,23]

The absorption coefficient α of external IR radiation can be expressed via the imaginary component of frequency-dependent dielectric permittivity $\varepsilon(\omega)$ in the following form:[24]

$$\alpha(\omega) = 2\frac{\omega}{c}\text{Im}\left[\varepsilon(\omega)^{1/2}\right].$$

In the case of depolarized light, the Raman spectrum $J(\omega)$ is specified by the following expression (the scatterings at $\omega < 0$ and $\omega > 0$ are of the Stokes and anti-Stokes types, respectively):[23]

$$J(\omega) = \frac{\omega}{(\omega_L - \omega)^4}\left(1 - \text{e}^{-\hbar\omega/kT}\right)\text{Re}\int_0^\infty \text{d}t\,\text{e}^{\text{i}\omega t}\left\langle \Pi_{xz}(t)\Pi_{xz}(0)\right\rangle,$$

where

$$\Pi(t) \equiv \sum_{j=1}^{N}\left[\alpha_j(t) - \left\langle \alpha_j \right\rangle\right],$$

ω_L is the exciting laser frequency, Π_{xz} is the xz component of the $\Pi(t)$ value, the x axis is directed along the molecular dipole, and xoy is the molecular plane. The value $\omega_L = 19436.3$ cm^{-1} (green line of argon laser, $\lambda = 514.5$ nm) has been used in the simulation.

Reflection coefficient R is determined as the ratio between the average energy flux reflected from a surface and the incident flux. At the normal incidence of a plane monochromatic wave, the reflection coefficient is determined by the following formula:[17]

$$R = \left| \frac{\sqrt{|\varepsilon_1|} - \sqrt{|\varepsilon_2|}}{\sqrt{|\varepsilon_1|} + \sqrt{|\varepsilon_2|}} \right|^2. \quad (1)$$

Here, it is assumed that the wave incidence occurs from a transparent medium (medium 1) into a medium that may be both transparent and nontransparent, i.e., an absorbing and scattering one (medium 2). The subscripts at the dielectric permittivity in Eq. (1) denote corresponding media.

The frequency dispersion of the dielectric permittivity determines the frequency dependence of dielectric loss $P(\omega)$ according to the following expression:[18]

$$P = \frac{\varepsilon'' \langle E^2 \rangle \omega}{4\pi},$$

where $\langle E^2 \rangle$ is the mean square electric field strength and ω is the frequency of the emitted electromagnetic wave.

The motions at frequencies below 1200 cm^{-1} correspond to molecular librations, while frequencies above 1200 cm^{-1} describe mainly intramolecular vibrations realized in the following approximation.[25] Flexible molecular models are considered. Molecules are provided with flexibility via the procedure developed within the framework of the Hamilton dynamics:[26–28] the deformation of a molecule is determined by equilibrating total potential force

$$\boldsymbol{f}(\boldsymbol{u}) = -\frac{\partial \boldsymbol{r}}{\partial \boldsymbol{u}} \nabla \Phi(\boldsymbol{r})$$

with centrifugal force $-\mu u \omega^2$, where μ is the reduced mass, u is the distance between two atoms, ω is the vibration frequency, and $\boldsymbol{r}$ determines the point at which the force is applied.

4. Results

As a result of adsorption of i methane molecules by a water cluster, a $(CH_4)_i(H_2O)_{50}$ cluster is formed. The configuration of a $(CH_4)_6(H_2O)_{50}$ cluster containing six CH_4 molecules at the 50-ps time moment is exemplified in Fig. 1. Methane molecules are arranged symmetrically with respect to the cluster center in the vertical and horizontal directions. They have rather arbitrary orientations that are determined by the positions and orientations of neighboring water molecules. As the tetrahedral CH_4 molecule carries external positive electric charges (on H atoms), the tetrahedron vertex is located closer to the negatively charged oxygen atom of a nearest water molecule. The situation, in which H atoms of methane molecule are located near O atoms of two or even three H_2O molecules, is also possible. The symmetrical arrangement of hydrophobic methane molecules results in the densification of the water component of the cluster, which affects its optical properties.

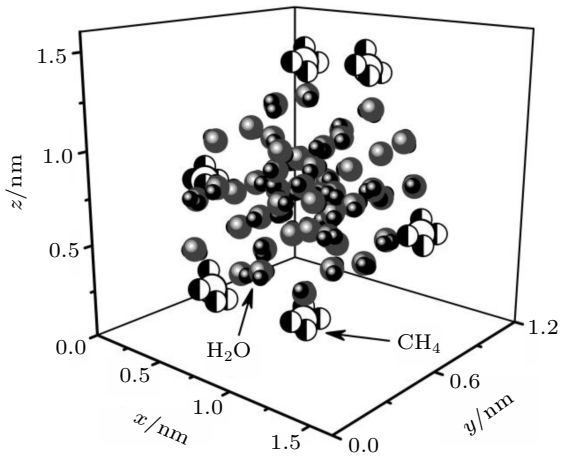


Fig. 1. Configuration of $(CH_4)_6(H_2O)_{50}$ cluster at the 50-ps time moment.

Figure 2 shows the frequency dependences of absorption coefficient α for systems I–III. The integral intensities of the $\alpha(\omega)$ spectra for these systems are related as 1:0.80:1.04. The main maxima of the spectra fall in the frequency range of 3270 cm^{-1}–3500 cm^{-1}. The $\alpha(\omega)$ spectra of liquid water[29] and an $H_2O/CH_4 = 20$ solid mixture at $T = 15$ K lie in the same range.[3] The IR absorption spectra of CH_4 and CD_4 captured in the matrix of an inert gas at low temperatures exhibit maxima the positions of 3015 cm^{-1} and 994 cm^{-1}, respectively.[30] The frequency range of 2750 cm^{-1} $\leq \omega \leq$ 3300 cm^{-1} is of particular importance, because it contains characteristic frequencies of stretching vibrations for molecules comprising carbon–hydrogen bonds. In the homologous series of hydrocarbons, the methane molecule is unique, because all C–H bonds belong to the same group, in contrast to, e.g., hexane, which comprises bonds of several types.

Figure 3 exhibits Raman spectra $J(\omega)$ calculated for systems I and III and the experimental spectrum of liquid water measured at 300 K.[31] The adsorption of CH_4 molecules by $(H_2O)_{50}$ clusters leads to a significant reduction in the number and intensity of the peaks. The comparison between the $J(\omega)$ spectra for system I and those for III shows that only a peak at 3117 cm^{-1} is well reproducible (with a weak blue shift). This peak exhibits a red shift (by ≈ 200 cm^{-1}) with respect to the main peak in the $J(\omega)$ spectrum of liquid water. In the case of pure water, different arrangements of oxygen

atoms with tetrahedral coordination and variability of hydrogen bond lengths and angles result in the formation of various ice phases. The incorporation of different guest molecules into the structural cavities of the polyhedral skeleton of water yields more than ten stable structures, which are divided into gas hydrates of three types denoted as sI, sII, and sH structures.[32] Pure methane hydrate forms, as a rule, a cubic sI structure, in which small methane molecules are easily accommodated in both large and small cavities. At pressures and temperatures higher than those for the sI structure, two other forms, sII and sH, are stable.[33] As a result of compression, methane hydrate sI is transformed into the sII phase at 100 MPa and, then, into the sH phase at 600 MPa. The Raman spectra of these different forms of methane hydrate are quite different (see the inset in Fig. 3). The main peaks of the three forms of methane hydrate show a red shift in the range of 200 cm^{-1}–213 cm^{-1} with respect to the main peak in the $J(\omega)$ spectrum of system III.

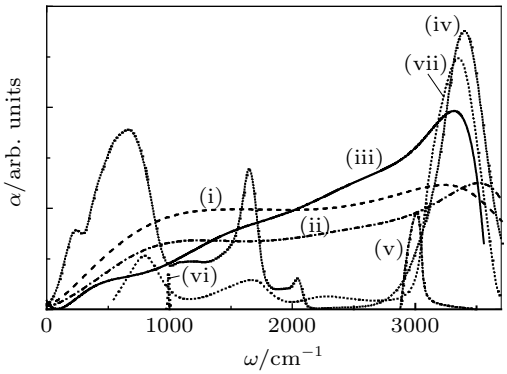


Fig. 2. Values of IR absorption coefficient $\alpha(\omega)$ for systems (i) I, (ii) II, and (iii) III; (iv) absorption coefficient experimentally determined for bulk liquid water;[29] absorption spectra of (v) CH_4 and (vi) CD_4 captured in an inert gas matrix;[30] and (vii) $\alpha(\omega)$ spectrum of solid mixture $[H_2O]/[CH_4] = 20$ at $T = 15$ K.[3]

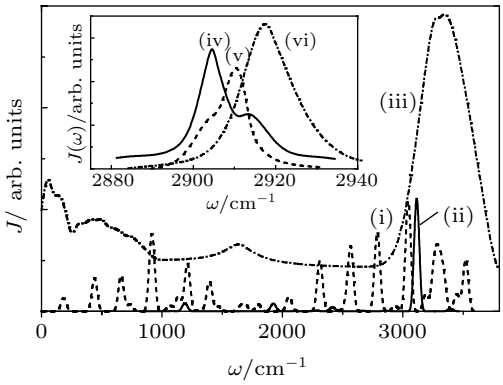


Fig. 3. Experimental Raman spectra for systems (i) I and (ii) III and (iii) liquid water at 293 K[31] and (iv)–(vi) experimental spectra of sI, sIII, and sH methane hydrates, respectively.[32]

The reflections of IR radiation by disperse systems I–III are characterized by the $R(\omega)$ spectra (Fig. 4). System II, which consists of water clusters with different sizes, has average reflection coefficient $\bar{R} = 0.35$ and frequency of most strongly reflected photons $\omega_R = 1015$ cm^{-1}. For system I, $\bar{R} = 0.41$ and $\omega_R = 976$ cm^{-1}, while, for system III, $\bar{R} = 0.74$ and $\omega_R = 3255$ cm^{-1}. Thus, the adsorption of CH_4 molecules by the system of clusters causes a 1.8-fold increase in reflection coefficient $\bar{R}$ and a considerable blue shift of the frequency of the most efficiently reflected radiation.

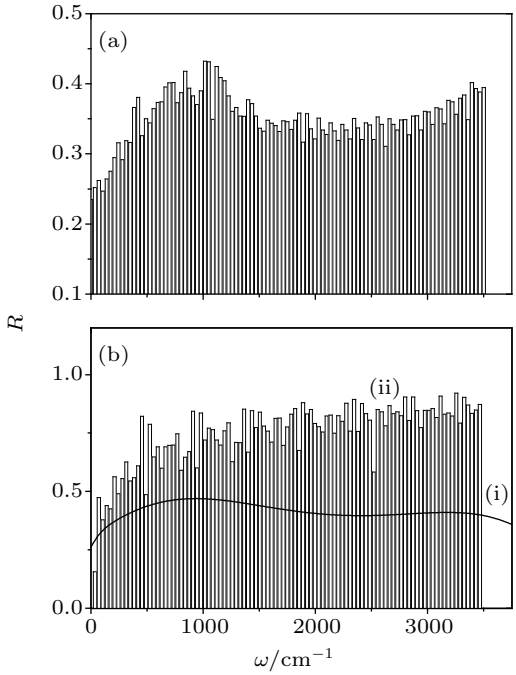


Fig. 4. Coefficients of monochromatic plane electromagnetic-wave reflection by different disperse systems: (a) II and (b) (i) I and (ii) III.

Figure 5 shows IR emission spectra $P(\omega)$ for systems I–III along with the laboratory emission spectrum of methane at 800 K.[34] The integral intensity ratio among the $P(\omega)$ spectra for systems I–III is 1:0.77:1.68, and the main peaks are positioned at 3340, 3471, and 3099 cm^{-1}. Thus, the addition of CH_4 molecules to $(H_2O)_{50}$ clusters is accompanied by a red shift of the main peak by 241 cm^{-1}. The position of the main peak for system III is in good accordance with that of the main peak of the experimental emission spectrum of methane (3087 cm^{-1}). Note that weak bands to the left and right of the $P(\omega)$ spectrum of methane (Fig. 5) were ignored in Ref. [34].

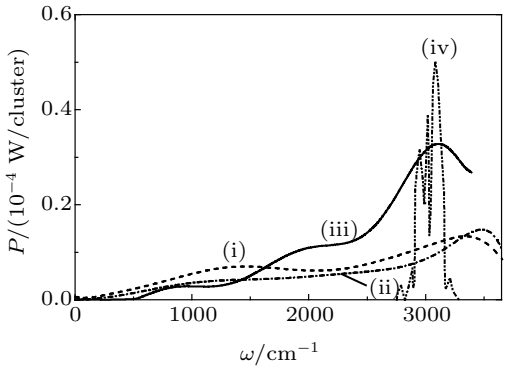


Fig. 5. IR emission spectra for systems (i) I, (ii) II, and (iii) III and (iv) emission spectrum of methane measured in laboratory experiments at 800 K.[34]

5. Conclusion

Methane adsorption by disperse aqueous medium is studied in terms of a molecular dynamics model of flexible molecules. An increase in the molar fraction of methane near a $(H_2O)_{50}$ cluster leads, in the long run, to the structurization of CH_4 molecules in the vicinity of the cluster. The integral absorption coefficient $\alpha(\omega)$ in the IR region increases with methane adsorption by the disperse aqueous medium. Therewith, the main absorption band shifts toward the position of the most intense band in the IR spectrum of gaseous methane. On the contrary, the number and intensity of bands dramatically decrease in the Raman spectrum of the disperse methane-containing system. In fact, only one meaningful band remains preserved in the $J(\omega)$ spectrum. As spherically symmetrical CH_4 molecules are adsorbed by the disperse aqueous system, its reflectivity noticeably increases and the frequency distribution of reflection coefficient becomes more uniform. The emission intensity of the water–methane disperse system markedly increases, especially in the high-frequency region of the $P(\omega)$ spectrum. The position of the main maximum in the $P(\omega)$ spectrum of this system is in good agreement with the position of the maximum in the emission spectrum of methane measured under laboratory conditions. Because of different selection rules, the calculated $\alpha(\omega)$ and $J(\omega)$ spectra may appear to be useful for the solution of some problems, including astrophysical ones.

References

[1] Boudon V, Rey M and Loete M 2006 *J. Quantum Spectrosc. Radiat. Transfer* **98** 394
[2] Roush T L 2001 *J. Geophys. Res.* **106** 33315
[3] Bernstein M P, Cruikshank D P and Sandford S A 2006 *Icarus* **181** 302
[4] Hudgins D M, Sandford S A, Allamandola L J and Tielens A G G M 1993 *Astrophys. J., Suppl. Ser.* **86** 713
[5] Laaksonen A and Stilbs P 1991 *Mol. Phys.* **74** 747
[6] Chandler D 2002 *Nature* **417** 491
[7] Chau P L and Mancera R L 1999 *Mol. Phys.* **96** 109
[8] Lambeth B P Jr, Junghans C, Kremer K, Clementi C and Delle Site L 2010 *J. Chem. Phys.* **133** 221101
[9] Galashev A Y 2010 *Mol. Simul.* **36** 273
[10] Galashev A E, Chukanov V N, Novruzov A N and Novruzova O A 2006 *High Temp.* **44** 364
[11] Galashev A E, Rakhmanova O R, Galasheva O A and Novruzov A N 2006 *Phase Transitions* **79** 911
[12] Dang L X and Chang T M 1997 *J. Chem. Phys.* **106** 8149
[13] Jorgensen W L and Madura J D 1983 *J. Am. Chem. Soc.* **105** 1407
[14] Galashev A E and Rakhmanova O R 2012 *Chin. Phys. B* **21** 113602
[15] New M H and Berne B J 1995 *J. Am. Chem. Soc.* **117** 7172
[16] Haile J M 1992 *Molecular Dynamics Simulation: Elementary Methods* (New York: Wiley) p. 160
[17] Landau L D and Lifshitz E M 1982 *Electrodynamics of Continuous Media* (Moscow: Nauka) p. 585
[18] Prokhorov A M 1988 *Physical Encyclopedia* (Moscow: Sovetskaya Entciklopediya) p. 702
[19] Koshlaykov V N 1985 *Problems of Solid Body Dynamics and Applied Theory of Gyroscopes* (Moscow: Nauka) p. 14
[20] Sonnenschein R 1985 *J. Comput. Phys.* **59** 347
[21] Bresme F 2001 *J. Chem. Phys.* **115** 7564
[22] Neumann M 1985 *J. Chem. Phys.* **82** 5663
[23] Bosma W B, Fried L E and Mukamel S 1993 *J. Chem. Phys.* **98** 4413
[24] Neumann M 1986 *J. Chem. Phys.* **85** 1567
[25] Stern H A and Berne B J 2001 *J. Chem. Phys.* **115** 7622
[26] Lemberg H L and Stillinger F H 1975 *J. Chem. Phys.* **62** 1677
[27] Rahman A, Stillinger F H and Lemberg H L 1975 *J. Chem. Phys.* **63** 5223
[28] Saint-Martin H, Hess B and Berendsen H J C 2004 *J. Chem. Phys.* **120** 11133
[29] Goggin P L and Carr C 1986 *Water and Aqueous Solutions* (Boston: Adam Hilger) p. 149
[30] Chamberland A, Belzile R and Cabana A 1970 *Can. J. Chem.* **48** 1129
[31] Vallee P, Lafait J, Ghomi M, Jouanne M and Morhange J F 2003 *J. Mol. Struct.* **651** 371
[32] Chou I M, Sharma A, Burruss C, Shu J, Mao H K, Hemley R J, Goncharov F, Stern L A and Kirby H 2000 *Proc. Natl. Acad. Sci. USA* **97** 13484
[33] Ripmeester J A, Ratcliffe C I, Klug D D and Tse J S 1994 *Ann. N. Y. Acad. Sci.* **715** 161
[34] Nassar R and Bernath P 2003 *J. Quantum Spectrosc. Radiat. Transfer* **82** 279